Withers, N. J., Howie, J., Hughes, J. M. O. & Robertson, P. K. (1989). *Géotechnique* **39**, No. 3, 433–454

Performance and analysis of cone pressuremeter tests in sands

N. J. WITHERS*, J. HOWIE†, J. M. O. HUGHES‡ and P. K. ROBERTSON†

This Paper presents the results of tests performed in sand with a prototype cone pressuremeter. Values of shear modulus and friction angle of the sand are derived from the data using cavity expansion/contraction theory. These values are compared with those obtained from seismic cone penetration tests and self boring pressuremeter tests. The Paper aims to stimulate the development of methods to evaluate and apply data obtained from tests in sands with this operationally convenient in situ test. The values of shear modulus obtained with the cone pressuremeter are compatible with those obtained from the other tests. The availability of a cone resistance profile provided by the cone pressuremeter, at the same location as the pressuremeter derived shear moduli, facilitates the production of a continuous depth profile of shear modulus based on a reliable site specific correlation. Available cavity expansion theory produces unrealistic values of peak friction and dilation angle from cone pressuremeter data. Available cavity contraction theory produces unrealistic values of friction and dilation angle from both cone pressuremeter and self boring pressuremeter data. Creep deformations contribute to the difficulties associated with the applications of cavity expansion and contraction theories. However, with appropriate test procedures the creep deformation can be identified. A standard test procedure is proposed to facilitate comparisons of data obtained from further tests in different sands. Such comparisons are needed to advance understanding of cone pressuremeter test data.

KEYWORDS: analysis; field tests; friction; sands; shear modulus site investigation.

L'article présente les résultats d'essais effectués dans du sable à l'aide d'un pressiomètre à cône prototype. Des valeurs du module de cisaillement et de l'angle de frottement du sable sont déduites de ces données par l'emploi de la théorie de l'expansion–contraction des cavités. Ces valeurs sont comparées avec celles obtenues à partir d'essais sismiques de pénétration au cône et d'essais au pressiomètre à autoforeur. Le but est de stimuler le développement de méthodes pour l'évaluation et l'application des données obtenues à partir d'essais effectués dans le sable à l'aide de cet essai in-situ très pratique. On en tire les conclusions suivantes: les valeurs du module de cisaillement obtenues par moyen du pressiomètre à cône sont compatibles avec celles obtenues à partir des autres essais; la production d'un profile continu de profondeur du module de cisaillement basée sur une corrélation spécifique et fiable est facilitée par la disponibilité d'un profil de résistance au cône fourni par le pressiomètre à cône au même emplacement que les modules de cisaillement dérivés du pressiomètre; la théorie actuelle de l'expansion des cavités donne des valeurs peu réelles du frottement de pic et de l'angle de dilatation à partier des données du pressiomètre à cône; la théorie actuelle de la contraction des cavités donne des valeurs peu réelles du frottement et de l'angle de dilatation à partir des données du pressiomètre à cône et du pressiomètre à autoforeur; les déformations par fluage augmentent les difficultés lorsque les théories de l'expansion et de la contraction des cavités sont employées, bien qu'il soit possible de définir la déformation par fluage à l'aide de procédures d'essais appropriées. L'article propose une procédure normale d'essai pour faciliter la comparaison des données obtenues à partir d'autres essais effectués dans des sables différents. De telles comparaisons sont nécessaires pour améliorer la compréhension des données des essais de pressiomètre à cône.

Discussion on this Paper closes 5 January 1990; for further details see p. ii.

* Formerly Fugro Geotechnical Engineers BV, Leidschendam, Holland; now Dames and Moore, Melbourne, Australia.
† University of British Columbia, Vancouver, Canada.
‡ Hughes Insitu Engineering Ltd, Vancouver, Canada.

NOTATION

Δ increment
ε strain at a point in soil (compression positive)
σ stress at a point in soil (compression positive)
Ψ inflation pressure inside pressuremeter
ξ pressuremeter strain $= (R - R_0)/R_0$
m parameter $= 1$ for cylindrical expansion–contraction
parameter $= 2$ for spherical expansion–contraction
r radius to a point in soil
R radius of pressuremeter
G shear modulus of soil
ϕ' peak angle of internal friction of soil
ϕ_{cv}' angle of internal friction when soil deforms at constant volume
ν angle of dilation of soil
n $(1 - \sin \nu)/(1 + \sin \nu)$
N $(1 - \sin \phi')/(1 + \sin \phi')$
N_{cv} $(1 - \sin \phi_{cv}')/(1 + \sin \phi_{cv}')$

Subscripts

0 initial condition
1 elasto-plastic boundary during expansion of cavity
2 elasto-plastic boundary during contraction of cavity
r radial direction
h hoop (circumferential) direction
m maximum value before start of unload–reload loop
e expansion, end of expansion
c contraction
ur unload–reload

Superscripts

L during expansion (loading) of pressuremeter

INTRODUCTION

The cone pressuremeter (Fig. 1) combines a 60° electric piezocone with the pressuremeter test. The prototype Fugro cone pressuremeter is described in detail in Withers, Schaap & Dalton, 1986. The pressuremeter module is the same diameter as the 43·7 mm dia. piezocone. The membrane has a length to diameter ratio of 10. Earlier examples of this type of pressuremeter are the full displacement pressuremeter (Hughes & Robertson, 1985) and the LPC pressiopenetrometer developed by Baguelin & Jezequel, (1983).

The full displacement pressuremeter consists of a 74 mm dia. self boring pressuremeter mounted directly behind a solid 60° tip and is pushed into the ground. The length to diameter ratio of the membrane is 6. The LPC pressiopenetrometer consists of an 89 mm dia. pressuremeter mounted behind an 89 mm dia. electric friction cone. It is vibrated into the ground. The length to diameter ratio of the pressuremeter is 4.

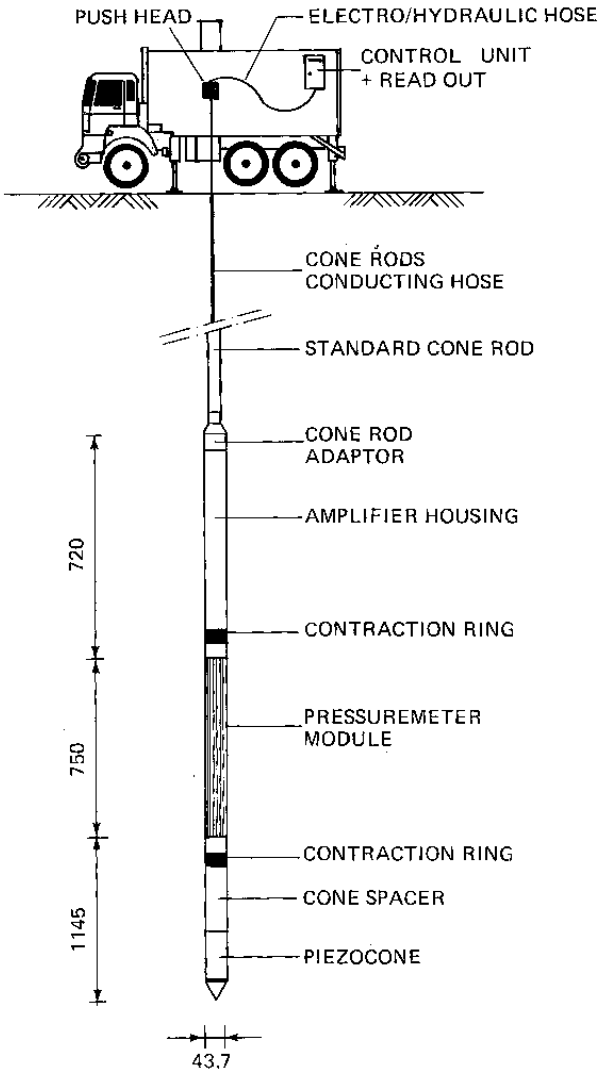

Fig. 1. Cone pressuremeter

The cone penetration test is now well established as a simple and relatively economical test which is of particular value in making detailed profiles of soil properties. Reasonably reliable classification of soils can be achieved with the use of published empirical correlations with the friction ratio and cone resistance measurements, as well as pore pressure measurements in the case of the piezocone. Absolute values of cone resistance can be used, again with empirical correlations, to estimate strength parameters in either sands or clays. The best results are obtained if site specific correlations, developed from laboratory or other in situ test (e.g. vane, pressuremeter) data are used. The cone resistance gives, however, only a poor indication of soil stiffness.

The pressuremeter is a device well suited to measuring both soil stiffness and strength parameters. The interpreted values of these parameters from tests in sand can be sensitive to soil dis-

turbance. Even with the self boring pressuremeter, it can be difficult to install the pressuremeter into heterogeneous soils with minimal and repeatable disturbance.

An alternative approach is to allow a repeatable amount of ground disturbance before the pressuremeter test. Good quality cone penetrometer tests produce repeatable values of cone resistance, sleeve friction and pore pressure when repeated tests are performed in the same soil at adjacent locations (Lunne *et al.* 1986). This suggests that the process of cone penetration disturbs the soil in a repeatable way. On this basis, it seems reasonable to expect that repeatable radial soil stresses would be developed on a pressuremeter which is driven or pushed behind a solid tip into the same soil at adjacent locations. These stresses could not be expected to equal the in situ horizontal stress. This type of pressuremeter will be described as a full displacement device to distinguish it from the self boring, Menard and other types of pressuremeter. The combination of the profiling ability of the piezocone with friction sleeve, together with the stress–strain measurements from the pressuremeter, in the form of the cone pressuremeter is a particular form of the full displacement type.

The new test is thus intended to add the ability to make accurate soil stiffness and strength measurements with the pressuremeter test to the operational convenience and soil profiling ability of the cone penetration test.

This Paper evaluates some tests made with the Fugro cone pressuremeter in sands. The values of shear modulus and friction angles obtained from the cone pressuremeter tests are compared with values obtained from self boring and full displacement pressuremeter tests and seismic cone penetration tests. The full displacement pressuremeter tests were performed with a self boring pressuremeter mounted behind a solid conical tip. The objectives of the comparisons are to explore the usefulness of this test, to comment on the suitability of available theoretical analyses and to propose a standard test procedure. The objectives of this Paper are to present data and to stimulate the development of methods to evaluate and apply data obtained with this potentially useful addition to techniques of in situ testing.

CONE PRESSUREMETER TESTS

A series of 25 cone pressuremeter tests were performed at the well documented University of British Colombia (UBC) research site at McDonald's Farm. The site is situated in the Fraser River delta of Vancouver, Canada, and comprises 2–3 m of compressible clays and silts overlying medium to coarse-grained sand with occasional thin layers of medium to fine sand and silty sand. The sand extends to a depth of 13–15 m. A cone penetration test (CPT) profile through the sand is shown in Fig. 2. Standard procedures were used for the cone penetration parts of the tests (i.e.

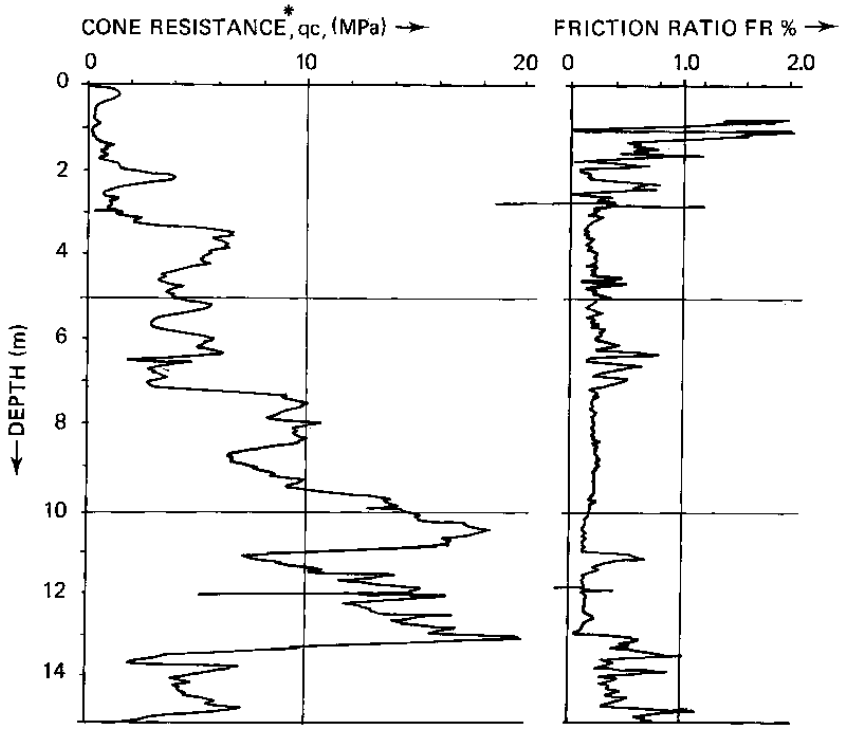

*(Note : from cone penetration test adjacent to cone pressuremeter test)

Fig. 2. CPT profile at McDonald's Farm

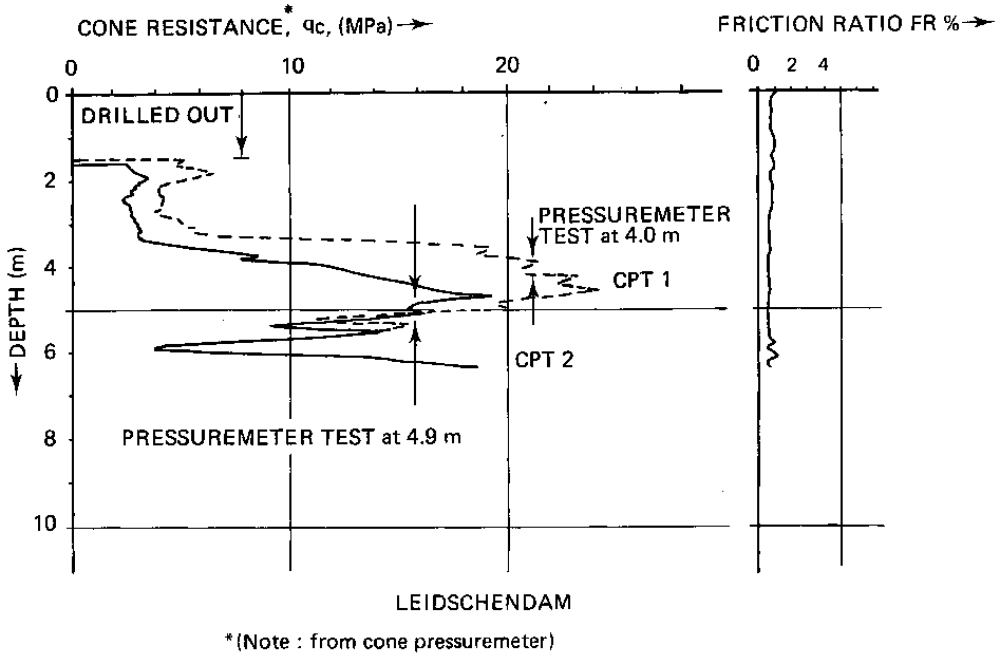

Fig. 3. CPY profile at Leidschendam

penetration rate of 2 cm/s). The sand is of variable density which tends to increase with depth. It is uniform with a D_{50} of 0·1 to 0·6 mm, and typically contains about 4% silt.

An additional six tests were carried out at Fugro's test site in Leidschendam, Holland, to provide independent confirmation in a similar sand of findings from the UBC tests. Again standard procedures were used for the cone penetration parts of the tests. The upper 6 m of the Leidschendam site comprise uniform beach sands. The D_{50} is about 0·17 mm and the silt content is in the range 0–1%. The cone resistance profile is summarized on Fig. 3. Fig. 4 presents the result of a typical cone pressuremeter test, in order to illustrate the test procedure.

The cone pressuremeter was stopped with the centre of the membrane at the depth (11·2 m in this case) selected from the cone resistance profile, and the thrust was removed from the cone rods. The inflation pressure was raised in increments until a radial displacement of about 5% was reached (A–B in Fig. 4). The pressure was held constant to allow creep to occur (B–C). A small unload–reload loop (C–D–C) was then performed, from which the elastic shear modulus could be evaluated. This procedure was repeated for larger radial displacements (EFGF and HIJ in

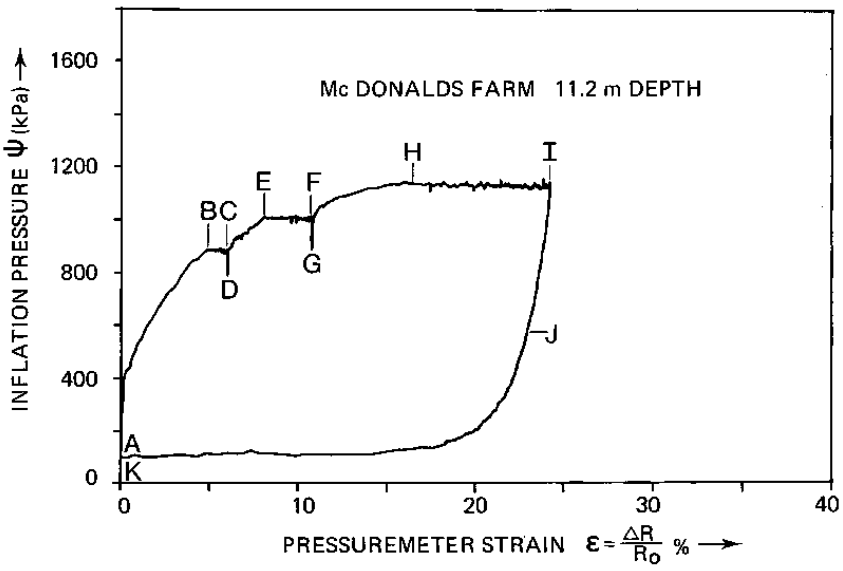

Fig. 4. Result of typical cone pressuremeter test

Fig. 4). From J, the membrane was fully unloaded to K in careful increments to obtain a complete unloading curve.

ANALYTICAL METHOD

The initial and dominant reason for developing the cone pressuremeter test for sands was to provide an in situ measurement of shear modulus which could be correlated with cone resistance. It was realized fundamental strength parameters (ϕ' and ν) would also need to be derived from the test results before the cone pressuremeter would achieve the widest acceptance and application. This requires an analysis which explains the pressure–expansion–contraction curve. Such an analysis needs to account for large strains, soil dilation, and the shape of the stress field around the pressuremeter both during cone penetration and during the pressuremeter test.

Available theoretical explanations of the mechanism of cone penetration in sand based either on bearing capacity or cavity expansion models do not accurately describe the distribution of stresses around a cone pressuremeter before it is inflated. Theoretical explanations of the mechanism of cone penetration in clay (Baligh, 1986) show that there is a narrow zone of intense deformation (compression under the cone tip and shear along its shaft) adjacent to the cone where shear strain levels and shear strain rates are extremely high. Outside this zone a larger zone of less intense plastic deformation exists, beyond which only elastic deformations occur.

It is plausible that an equivalent zone of intense deformation also exists adjacent to a cone penetrating sand. High shear strains and high shear strain rates imply that discrete shear planes or discontinuities may develop in this zone. This may explain why neither bearing capacity, nor cavity expansion theories, can model accurately the patterns of soil displacements and stresses around the penetrating cone pressuremeter before expansion of the membrane.

Hughes & Robertson (1985) have presented a plausible qualitative description of the stress paths followed by soil elements at different radii during expansion of the cone pressuremeter. They suggest an arch of high mean effective stresses is probably generated between the elastic and intense deformation zones. They also explain how the initial part of the pressure expansion curve is unlikely to be suitable for analysis using simple cavity expansion theories because the pattern of mean effective stresses at different radii is likely to be complex. This means that the stiffness and yield stress of soil elements will also vary with radius in a complex manner. At sufficiently large expansions it is possible that this complex pattern of stresses would be erased and replaced by a simpler pattern. In such a case, the pressuremeter data might be more amenable to interpretation using available cavity expansion–contraction theory based on uniform soil conditions before the start of membrane expansion.

Erasure of the complex stress history from cone penetration would mean that the maximum previous mean effective yield stress of every soil element inside the elastic plastic boundary would need to be exceeded with the radial effective stress re-established as the major principal stress.

The successful use of cavity expansion/contraction analysis of cone pressuremeter tests in clay (Houlsby & Withers, 1987) also suggested it would be worthwhile to examine the suitability of equivalent analyses for tests in sand. This examination consisted of three parts.

In the first, the shear modulus calculated from the slope of small unload–reload reload loops has been plotted against the radial expansion of the membrane at which the loops were made. If the previous stress history is erased successfully, then the shear modulus should decrease to a minimum value as the stiffening effect of the soil arch created by cone penetration is removed. Thereafter it should increase again (similar to the observed response to self boring pressuremeter tests) as the increased mean effective stresses in the zone of plastic deformations become more important.

Secondly, the pressure–expansion curves were plotted on logarithmic scales to investigate if asymptotes to straight lines could be found at high expansions. The slopes of these straight lines were converted to friction angles using cavity expansion theory (Hughes, Wroth & Windle, 1977) and compared with values obtained from self boring and full displacement pressuremeter tests at similar depths.

In the third part, the pressure–contraction curves were also plotted on logarithmic scales and the slopes of asymptotic lines converted to friction angles using cavity contraction theory (Houlsby, Clarke & Wroth, 1986) and compared with values similarly obtained from self boring and full displacement pressuremeter tests.

At large membrane expansions the boundary between the elastically and plastically deforming regions may have a diameter comparable with the length of the pressuremeter. Therefore, as the membrane expands, it is possible that the deformation pattern may progress from a cylindrical to a spherical shape and spherical cavity expansion theory may be more appropriate for modelling the later part of an expansion test.

In the following sections, the solutions, from available analyses, for both cylindrical and spherical cases are presented together so that the two interpretations may be compared.

ELASTIC–PLASTIC BOUNDARIES DURING CAVITY EXPANSION AND CONTRACTION

The stages of the pressuremeter test are shown schematically in Fig. 5. Point A is initially at the centreline of the pressuremeter before installation, (Fig. 5(a)). After installation A is at radius R_0, the original pressuremeter radius, (Fig. 5(b)). The pressuremeter is then expanded so that its radius R is $R_0 < R < R_e$. R_e is the maximum radius reached during expansion, (Fig. 5(c)). Fig. 5(d) shows A at a radius R_c ($R_0 < R_c < R_e$) during the contraction phase.

Point E lies on the elastic–plastic boundary at the maximum expansion and is then at radius r_1 (Fig. 5(c)). Initially point E was at r_e. Point C lies on the elastic–plastic boundary which is at radius

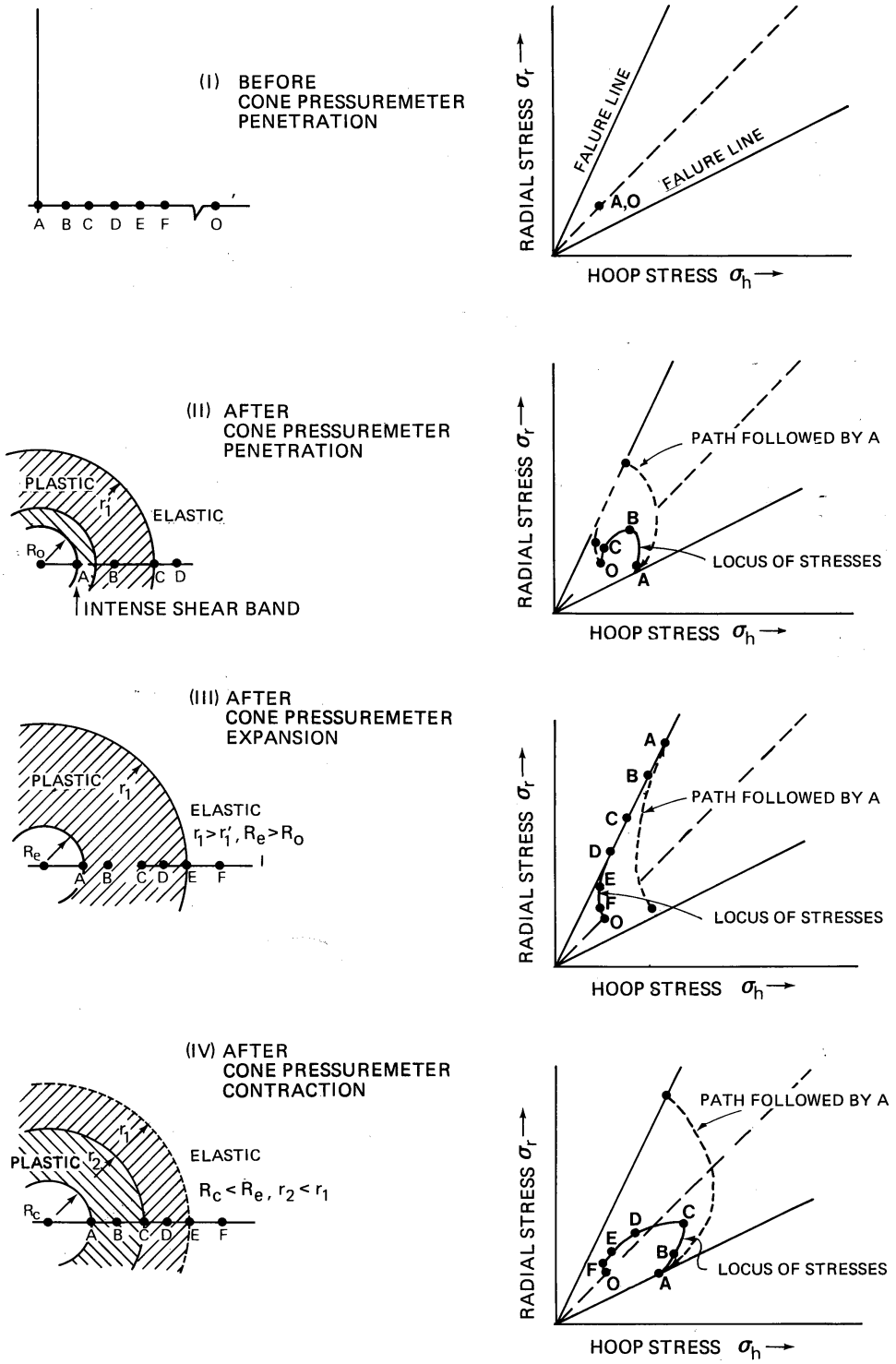

Fig. 5. Elastic–plastic boundaries and stress paths during cone pressuremeter test

r_2 when the pressuremeter has contracted to radius R_c. When the pressuremeter radius was R_e, point C was at a larger radius r_c.

During expansion the elastic–plastic boundary has radius r, which increases from the radius of the membrane R ($>R_0$), after initial yield, to the radius r_1 when the membrane has expanded to radius R_e.

During contraction, the elastic–plastic boundary has radius r which increases from the radius of the membrane R ($<R_e$) to r_2 when the membrane has contracted to radius R_c. Thus the material between R and r_2 has been loaded plastically and then unloaded so that reverse plasticity has occurred. The material between r_2 and r_1 has been loaded plastically and unloaded elastically. The material outside r_e has been loaded and unloaded elastically.

AVAILABLE CAVITY EXPANSION EQUATIONS

The well known equations for cylindrical cavity expansion (Hughes *et al.*, 1977) are restated here in a more general form which accommodates spherical cavity expansion. They presume that a cavity has been expanded from an initial radius R_0 in a frictional material in which the radial and hoop stresses were initially equal (and $K_0 = 1{\cdot}0$ for the spherical analysis).

In the elastic zone ($r > r_1$)

$$\sigma_r = \sigma_{r0} - 2mG(\varepsilon_h) \tag{1}$$

At the elastic–plastic boundary, ($r = r_1$)

$$\sigma_{r1} = \left[\frac{1+m}{1+mN}\right]\sigma_{r0} \tag{2}$$

$$\varepsilon_{h1} = -\frac{\sigma_{r0}}{2G}\frac{(1-N)}{(1+mN)} \tag{3}$$

In the plastic zone ($R < r < r_1$)

Defining, $\Delta\varepsilon_r/\Delta\varepsilon_n = -n$ and $\sin v = -$ [increment of volumetric strain/increment of shear strain] (Rowe, 1962), one derives

$$\sin v = -\left[\frac{\Delta\varepsilon_r + m\Delta\varepsilon_h}{\Delta\varepsilon_r - \Delta\varepsilon_h}\right] = \frac{m-n}{1+n} \tag{4}$$

$$n = \frac{m - \sin v}{1 + \sin v} \tag{4a}$$

$$\frac{\sigma_r}{\sigma_{r1}} = \left[\frac{r}{r_1}\right]^{-m(N-1)} = \left[\frac{(1+n)(\varepsilon_h/\varepsilon_{h1}) + m - n}{1+m}\right]^{m(1-N)/(1+n)} \tag{5}$$

$$\frac{\sigma_r}{\sigma_{r0}} = \left[\frac{1+m}{1+mN}\right] \times \left[\frac{(2G/\sigma_{r0})(1+n)(1+mN)\varepsilon_h}{(1+m)(1-N)} + \frac{(m-n)(1-N)}{(1+m)(1-N)}\right]^{m(1-N)/(1+n)} \tag{6}$$

Equation of pressure expansion curve

Cylindrical expansion

$$\frac{\Psi}{\sigma_{r0}} = \left[\frac{2}{1+N}\right] \times \left[(G/\sigma_{r0})(1+n)\frac{(1+N)}{(1-N)}\xi + \frac{(1-n)}{2}\right]^{(1-N/1+n)} \tag{7}$$

Spherical expansion

$$\frac{\Psi}{\sigma_{r0}} = \left[\frac{3}{1+2N}\right]\left[\frac{(2G/\sigma_{r0})(1+n)(1+2N)}{3(1-N)}\xi + \frac{(2-n)}{3}\right]^{2(1-N)/(1+n)} \tag{7a}$$

Unload–reload loops

$$\Delta\Psi = 2mG\Delta\xi/(1+\xi_m) \tag{8}$$

AVAILABLE CAVITY CONTRACTION EQUATIONS

The method of Houlsby *et al.* (1986) is followed except that the equations are developed for cylindrical and spherical displacements. The maximum inflation pressure and pressuremeter strain (negative hoop strain at the pressuremeter surface) at the end of the expansion phase are Ψ_e and ξ_e respectively.

Elastic phase

The soil behaves elastically during the initial phase of cavity contraction, with elastic unloading of the previously plastic section. The elastic phase ends when

$$\Psi = N\Psi_e \tag{9}$$

$$\xi = \xi_e - \frac{(1-N)\Psi_e}{2mG} \tag{10}$$

Elastic–plastic boundary ($r = r_2$)

On further unloading, a zone of soil in which reverse plasticity occurs spreads out from the pressuremeter. The following equations can be developed for the radial stress, and the radial and the hoop strains at this new elastic–plastic boundary

$$\sigma_{r2} = N\sigma_{r1}^{L}\left|\frac{r_2}{r_1}\right|^{m(N-1)} \tag{11}$$

$$\varepsilon_{h2} = \frac{\varepsilon_{h1}}{1+n}\left[(n-m) + (1+m)\left(\frac{r_2}{r_1}\right)^{-(n+1)} - \frac{(1+m)(1+n)}{m}\left(\frac{r_2}{r_1}\right)^{m(N-1)}\right] \tag{12}$$

It should be noted that

$$\sigma_{r1}^{L} = \left[\frac{1+m}{1+mN}\right]\sigma_{r0} \tag{13}$$

$$\varepsilon_{r2} = \frac{\varepsilon_{h1}}{(1+n)}\left[-(m+n) - n(m+1)\left(\frac{r_2}{r_1}\right)^{-(n+1)} + (1+m)(1+n)\left(\frac{r_2}{r_1}\right)^{m(N-1)}\right] \tag{14}$$

Within reverse plasticity zone ($R \leqslant r \leqslant r_2$)

Solution of the equilibrium equation gives

$$\left[\frac{r_2}{R}\right] = \left[\frac{\Psi}{N\Psi_e}\right]^{[N/m(N^2-1)]} \tag{15}$$

Solution of the compatibility equation gives

$$\left(\frac{r_2}{R}\right)^{[((nMN+1)/n)+(1-m)]} = \left[\frac{(2G/\Psi_e)(\xi_e - \xi)(m)[(1+nmN)+n(1-m)]}{(1-N)[(1-m)(1+n)+nm(m+N)]} + \frac{-(1-N)(1-nm)(m)}{(1-N)[(1-m)(1+n)+nm(m+N)]}\right] \tag{16}$$

Equation of pressure contraction curve

Combining the last two equations gives the equation of the pressure contraction curve

$$\frac{\Psi}{N\Psi_e} = \left[\frac{(2G/\Psi_e)(\xi_e - \xi)(m+nm^2N) + nm(1-m) - (1-N)(m-nm^2)}{(1-N)[(1-m)(1+N)+nm(m+N)]}\right]^{[nm(N^2-1)/(nmN^2+N)+nN(1-m)]} \tag{17}$$

This is the same as the result obtained by Houlsby *et al.* (1986) except that N was incorrectly stated in this Paper (Houlsby, private communication).

Cylindrical contraction

Putting $m = 1$ for the cylindrical case gives

$$\frac{\Psi}{N\Psi_e} = \left[\frac{(2G/\Psi_e)(\xi_e - \xi)(1+nN)}{(1-N)(1+N)n} - \frac{(1-N)}{(1+N)n}\right]^{n(N^2-1)/(nN^2+N)} \tag{18}$$

Spherical contraction

Putting $m = 2$ for the spherical case gives

$$\frac{\Psi}{N\Psi_e} = \left[\frac{(2G/\Psi_e)(\xi_e - \xi)[(2+4nN)-2n]}{1-N[2n(2+N)-(1+N)]} \frac{-(2-4N)}{[2n(2+N)-(1+N)]}\right]^{[2n(N^2-1)/2N^2n+N-nN]} \tag{18a}$$

EVALUATION OF SHEAR MODULUS FROM PRESSUREMETER DATA

Current practice for measuring shear modulus applies small strain elastic theory to small unload–reload loops. It is not obtained from the pressure–expansion curve. It has been found that

(*a*) the loop remains sensibly linear provided the unloading is not sufficient to cause failure in extension (Wroth, 1982; Hughes, 1982)

(*b*) the loop can show apparent large hysteresis unless excess pore pressures generated during inflation are allowed to dissipate, and also most potential creep strains are allowed to occur, before the unload–reload loop is made (Hughes, 1982)

The modulus was calculated from the slope of the unload–reload loops using the following expression

$$G = (\Delta\Psi/2\Delta\xi)(1+\xi_m) \tag{19}$$

(from equation (8)).

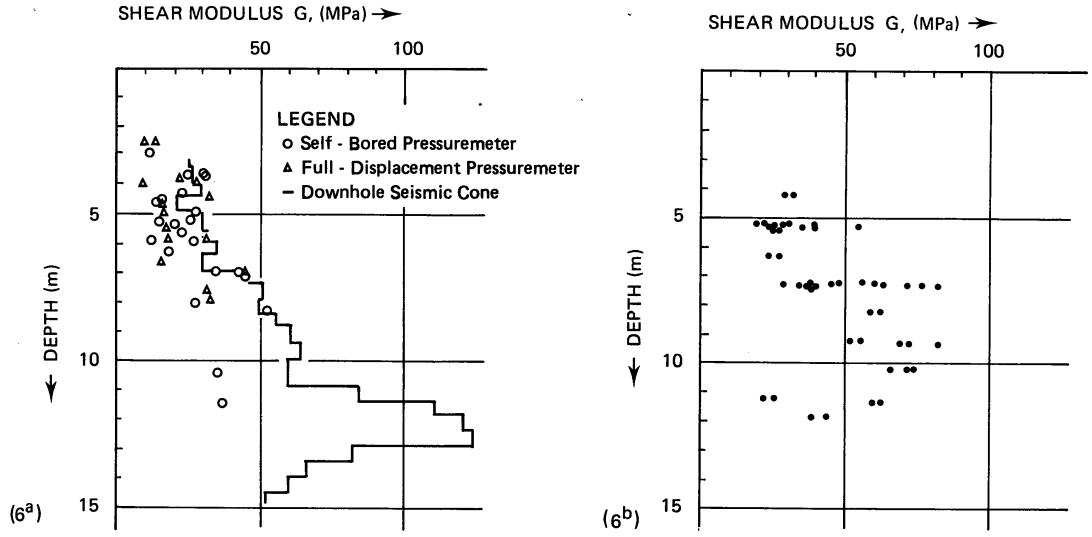

Fig. 6. Shear moduli at McDonald's Farm (a) other pressuremeter and seismic cone data (Hughes & Robertson, 1985); (b) cone pressure data

The term $(1 + \xi_m)$ accounts for the initial displacement before unloading. It has been commonly ignored in analyses of pressuremeter tests for which ξ_m is typically less than 10%.

Figure 6 shows that the shear moduli obtained with the cone pressuremeter compare well with earlier published data from self boring pressuremeter, full displacement pressuremeter and seismic cone at tests McDonald's Farm. This is encouraging considering the large disturbance

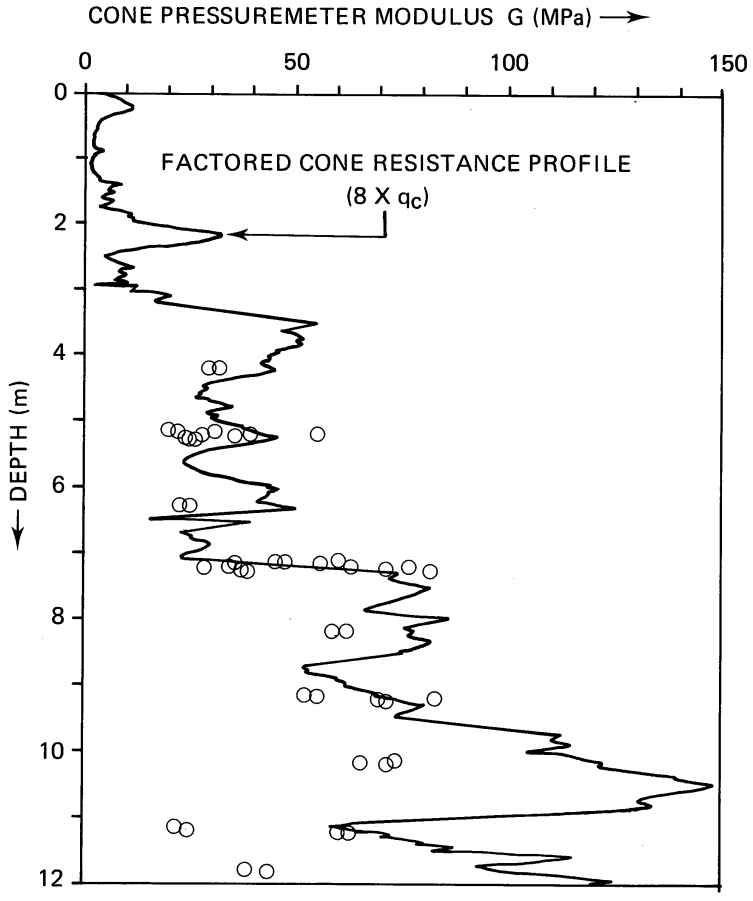

Fig. 7. Example of correlation of shear modulus with cone resistance

caused by the cone penetration. It tends to confirm

(*a*) the correctness of the assumption of cylindrical increments of displacements
(*b*) the observation, by Hughes & Robertson (1985), of the similarity of moduli measured with the seismic cone, the full displacement pressuremeter and the self boring pressuremeter.

Figure 7 demonstrates how the cone pressuremeter can be used conveniently to generate a continuous profile of shear modulus with depth at McDonald's Farm. A correlation of $G = 8\ q_c$, where q_c is the cone resistance, was used in this case.

The natural variability of the sand at McDonald's Farm, which has been observed previously (Hughes & Robertson, 1985), emphasizes the potential importance, even for this well documented site, of correlating the pressuremeter shear moduli G with a cone resistance q_c from the same borehole.

It is widely accepted that soil shear modulus depends on the current mean effective stress and on previous stress history. Laboratory research currently in progress will assess the effect of these factors on the modulus measured with a cone pressuremeter. Other factors which may affect the value of shear modulus measured by a pressuremeter include

(*a*) pressuremeter strain at the start of unloading
(*b*) size of unload strain increment
(*c*) creep rate at the start of unloading

The data obtained at McDonald's Farm and Leidschendam illustrates qualitatively the effect of these factors.

Influence of pressuremeter strain

Figure 8 shows the results of pressuremeter cone tests at McDonald's Farm and at Leidschendam, in which several unload–reload loops were made. The variation of the modulus G with the pressuremeter strain at the start of unloading ξ_m is shown in Fig. 9.

The pattern shown in Fig. 9 remains to be further investigated and explained. It is suggested that the initial peak at around $\xi_m = 2\%$ may reflect the stiffening effect of an annular zone of high mean effective stresses set-up by cone penetration (Hughes & Robertson, 1985). At larger pressuremeter strains the sand in this annular zone yields and the slopes of unload–reload loops may reflect the proportionally greater influence of the sand beyond, in which lower mean effective stresses exist. Similar plateau values of shear modulus were achieved after about $\xi_m = 10\%$ (Fig. 9(b)) in two tests from 4·0 and 4·9 m depth at Leidschendam.

If further tests in different soils were to confirm that plateau values were a consistent feature of cone pressuremeter tests, then it would suggest the following.

(*a*) The plateau value may be a repeatable measurement in separate tests in the same soil. Further tests are needed in a range of different soils to confirm this.
(*b*) The test procedure needs to be designed to demonstrate plateau values of G have been obtained. This implies load–unload loops need to be performed at more than one membrane expansion.
(*c*) A repeatable plateau value may either represent the undisturbed in situ shear modulus, or be suitable for correlation with the undisturbed in situ shear modulus.

Size of unload strain increment and creep rate at start of unloading

The order of size of the pressuremeter strain increment over the whole loop is $\Delta\xi = 0{\cdot}1\%$ (equivalent to $\Delta R = 0{\cdot}02$ mm). This implies that, for optimally accurate measurement of the slope of the unload loop, a resolution in the measurement of ξ better than 0·02% ($\Delta R = 0{\cdot}004$ mm) is needed. This is equivalent to 1 part in 2500 of a full-scale pressuremeter strain of $\xi = 50\%$. The resolution of displacement measurement is affected by such factors as hysteresis, repeatability, linearity and stability of the displacement sensor signal. It is clear that, to measure shear moduli with high accuracy in sand, close attention to these factors is necessary in the design of pressuremeters.

The resolution of unload–reload data obtained with prototype cone pressuremeter was adversely affected by some friction in the displacement sensors. This has contributed to the scatter in the data. This prevents any quantitative conclusions being drawn concerning the influence of creep rate and strain increment. Nevertheless, inspection of the data suggests that creep rate and strain increment size have had only a secondary influence on the shear moduli determined for the McDonald's Farm and Leidschendam sands.

It is hoped that improvements incorporated in succeeding generations of cone pressuremeters will produce data of sufficient accuracy so that the sensitivity of the modulus both to the size of the elastic strain increment in the unload–reload loop, and the creep rate before unloading can be quantified reliably.

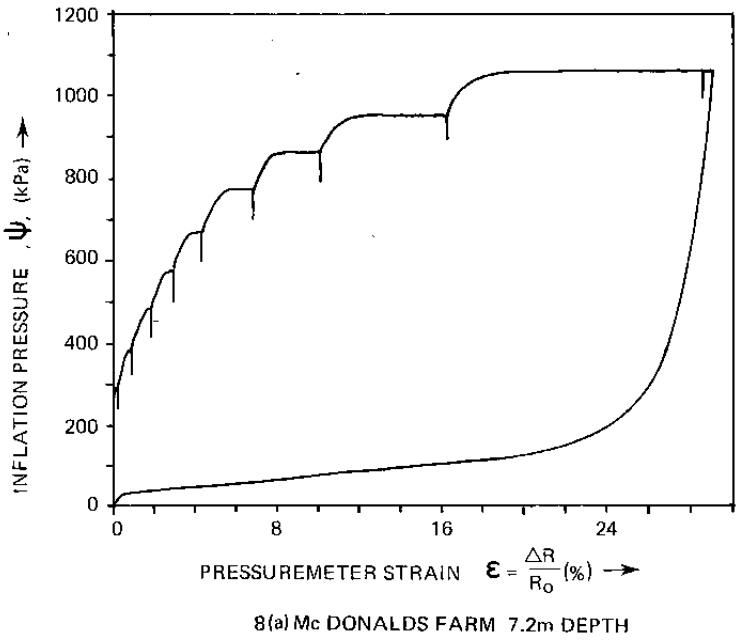

8(a) Mc DONALDS FARM 7.2m DEPTH

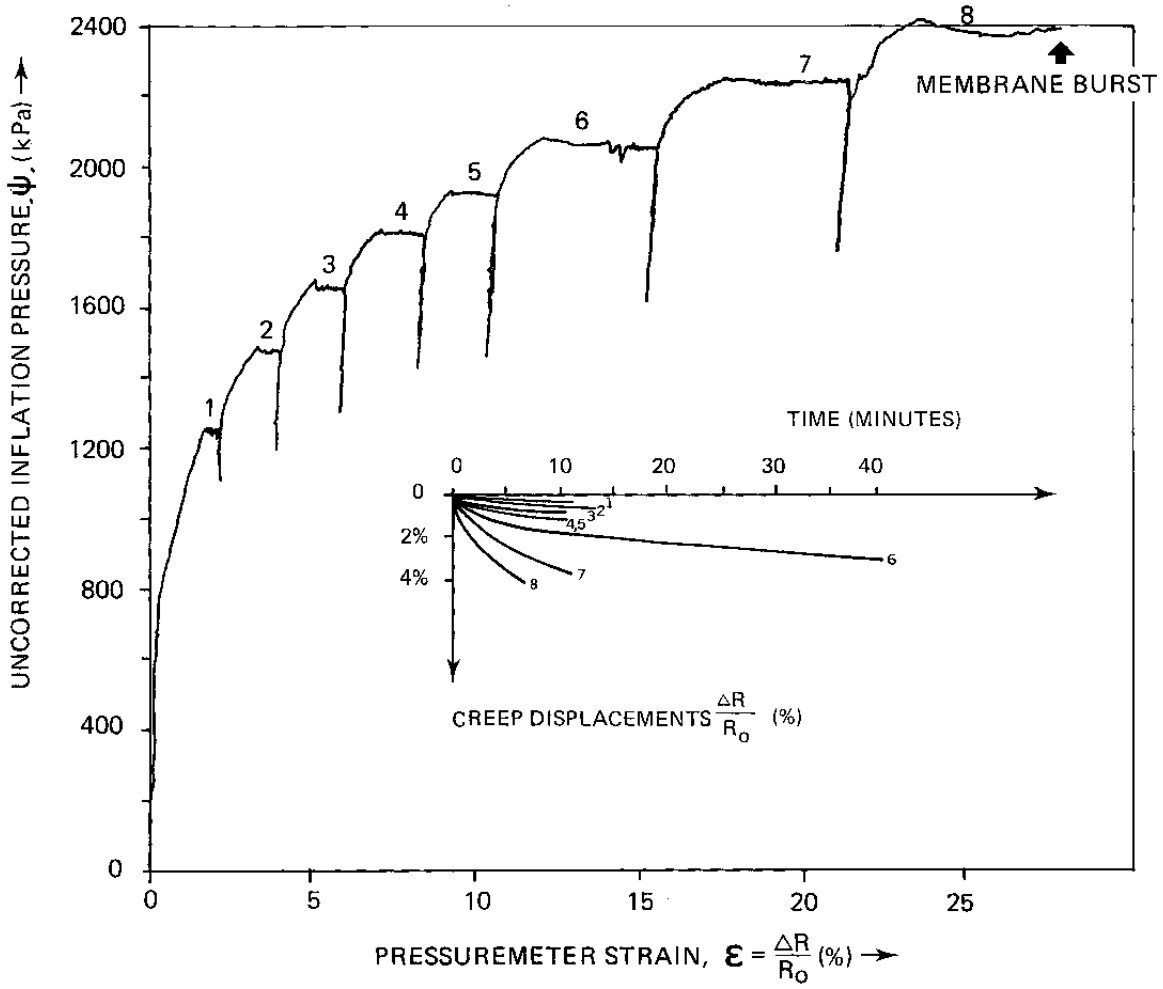

8(b) LEIDSCHENDAM 4.9 m

Fig. 8. Cone pressuremeter tests with several unloading loops: (a) McDonald's Farm, at 7·2 m depth; (b) Leidschendam, at 4·9 m depth

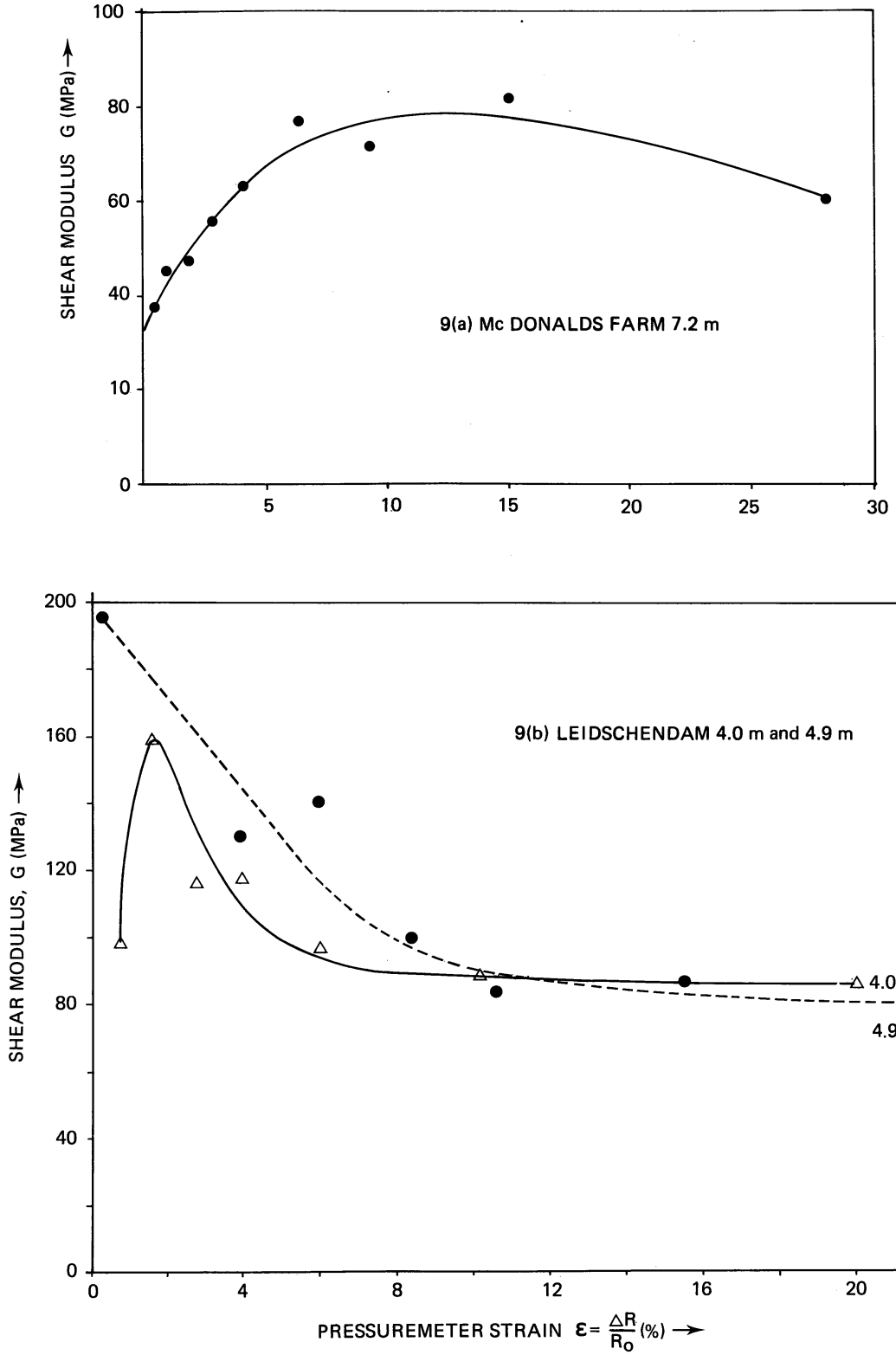

Fig. 9. Variation of shear modulus with pressuremeter strain before unloading: (a) McDonald's Farm, 7·2 m; (b) Leidschendam, 4·0 and 4·9 m

EVALUATION OF FRICTION ANGLE FROM CONE PRESSUREMETER DATA

The conventional cavity expansion–contraction analyses presented above lend themselves to graphical methods of calculating friction angle (Hughes *et al.*, 1977). These methods will be used to evaluate the suitability of these analyses for deriving angles of internal friction from cone pressuremeter data.

Derivation from pressure–expansion curves

It can be shown that the analytical expression for the expansion curve (equations (7) and (7a)) can be written in the form

$$\log \Psi = S_e \log (\xi + c_e) + \text{constant} \quad (20)$$

It can also be shown that the constant c_e is negligibly small compared with ξ for a wide range of soil properties. Therefore, the slope of a plot of $\log \Psi$ against $\log \xi$ should asymptote to slope S_e, where

$$S_e = (\Delta \log \Psi)/(\Delta \log \xi) \quad (21)$$

$$= \frac{1 - N}{1 + n} \text{ for cylindrical expansion} \quad (21a)$$

$$= \frac{2(1 - N)}{1 + n} \text{ for spherical expansion} \quad (21b)$$

Derivation from pressure–contraction curves

It can be shown that the analytical expression for the contraction curve (equations (18) and (18a)) can be written in the form

$$\log_e \frac{\Psi}{\Psi_e} = S_c \log_e \left[\frac{(\xi_e - \xi)}{(1 + \xi_e)} + c_c\right] + \text{constant} \quad (22)$$

It can also be shown that the constant c_c is negligibly small compared with $(\xi_e - \xi)/(1 + \xi_e)$ for a wide range of soil properties. Therefore, the slope of a plot of $\log \Psi/\Psi_e$ against $(\xi_e - \xi)/(1 + \xi_e)$ should asymptote to slope S_c where

$$S_c = (\Delta \log (\Psi/\Psi_e)) \Big/ \Delta \log_e \left(\frac{\xi_e - \xi}{1 + \xi_e}\right) \quad (23)$$

$$= \frac{n(N^2 - 1)}{(nN^2 + N)} \text{ for cylindrical contraction} \quad (23a)$$

$$= \frac{2n(N^2 - 1)}{(2N^2 n + N - nN)} \text{ for spherical contraction} \quad (23b)$$

The parameters can be related using

$$N = nN_{cv} \quad (24)$$

Therefore the angle of dilation v and the angle of friction ϕ' can be determined from the measured value of the slopes S_e or S_c and an assumed value of the angle of friction ϕ_{cv}' for constant volume deformations.

Selection of slopes S_e, S_c

Figure 10 summarizes self boring, full displacement and cone pressuremeter curves from about 5·0 m depth at McDonald's Farm. Figs 11 and 12 show the expansion and contraction curves plotted on logarithmic scales. They provide a measure of the repeatability of the data. The natural variability of the sands at 5·0 m depth at McDonald's Farm is shown by variations in cone resistance q_c at this depth (from Fig. 14 in Hughes & Robertson (1985) of between 2·5 and 7·0 MPa. This variability severely limits any expectations for identical data from several tests by any one type of pressuremeter at the same depth.

The slopes S_e, S_c were selected having regard to the following.

(*a*) The theory which suggests that the plotted curve should asymptote to a straight line as pressuremeter strain increases.

(*b*) The evidence of the increasing importance of creep deformations at larger pressuremeter strains and pressures (Fig. 8(a), (b)) suggests that at higher pressuremeter strains the plotted curve would deviate below the theoretical straight line. Evidence of this can be seen in Fig. 11(c).

(*c*) Creep deformations affect the value of ξ_e at the end of inflation. True values of S_c will be large (more negative) than those calculated. However, the value of ξ_e was not corrected because no systematic method of doing so was apparent. Values of ϕ' will therefore be underestimated.

Therefore the best straight line fit to the middle portion of expansion curves was selected to determine S_e.

No such phenomenon appears to be affecting the deflation curves and the selection of the slopes S_c from Fig. 12 was straightforward.

Evaluation of friction angle

Figures 13 and 14 are nomograms from which the friction angle ϕ' and dilation angle v can be obtained. Superimposed on these nomograms are the slopes obtained from the logarithmic plots.

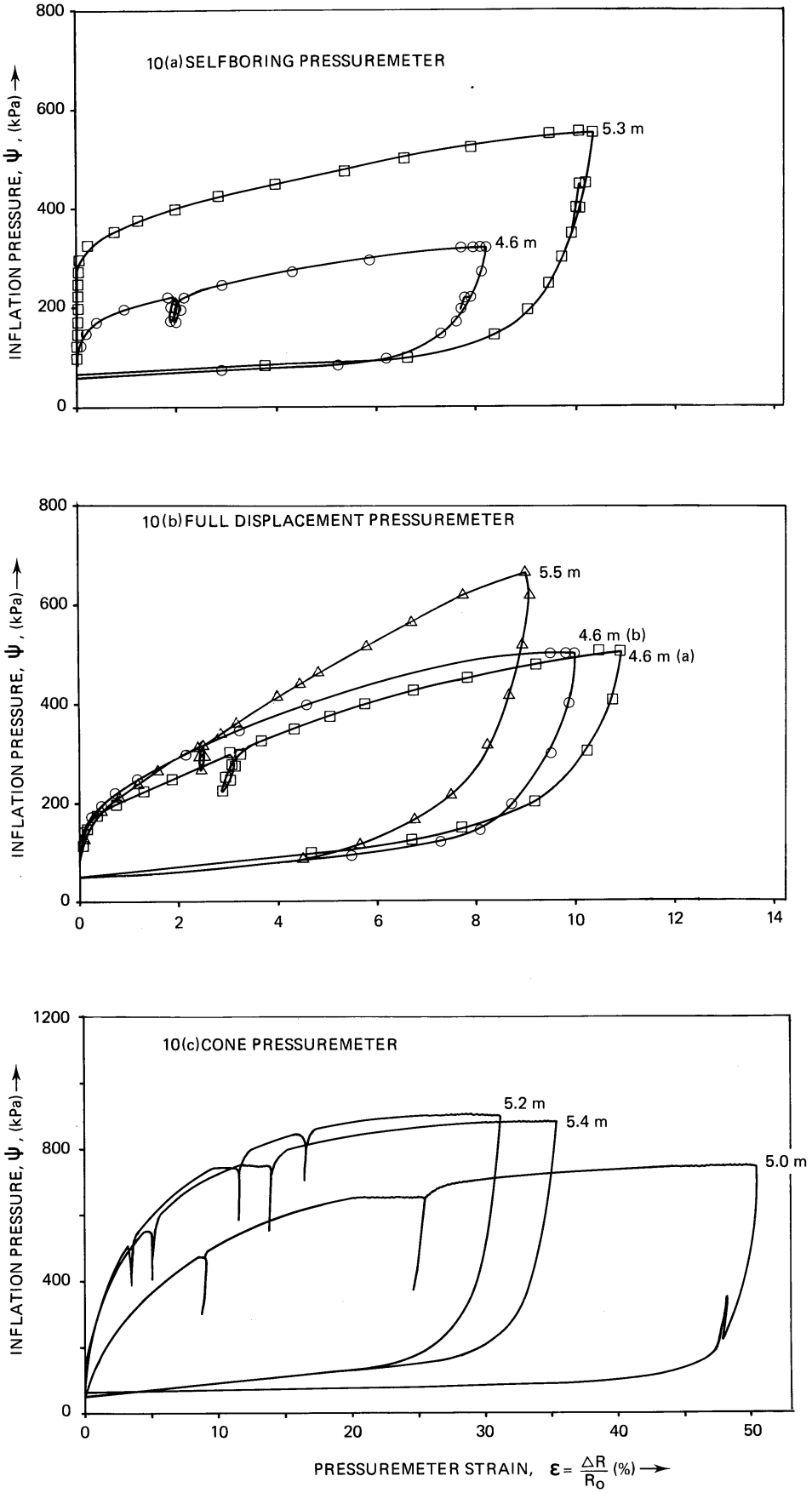

Fig. 10. Comparison of pressuremeter tests at 5 m depth at McDonald's Farm: (a) self boring; (b) full displacement; (c) cone

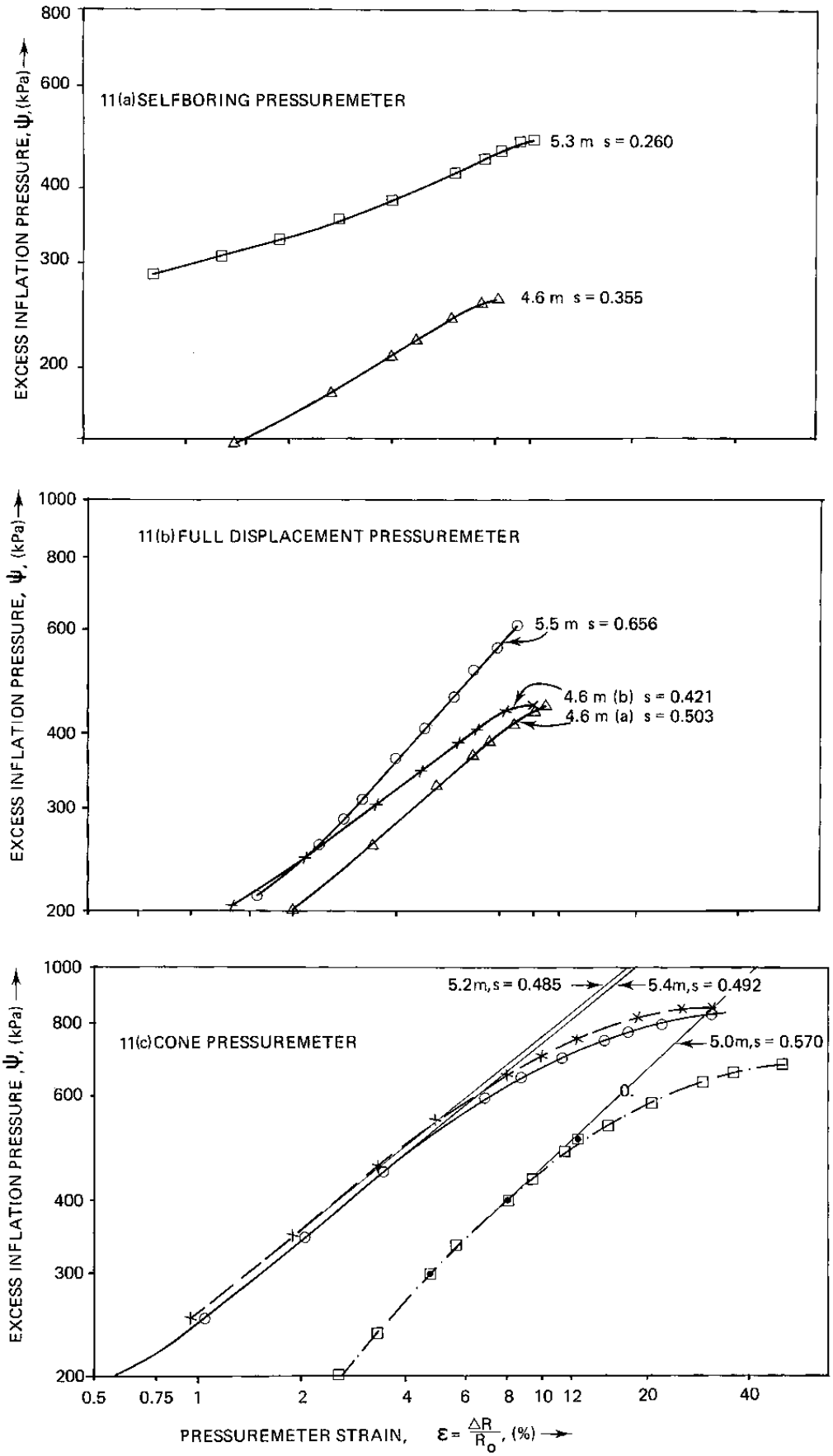

Fig. 11. Analysis of expansion data from pressuremeter tests at 5 m depth at McDonald's Farm: (a) self boring; (b) full displacement; (c) cone

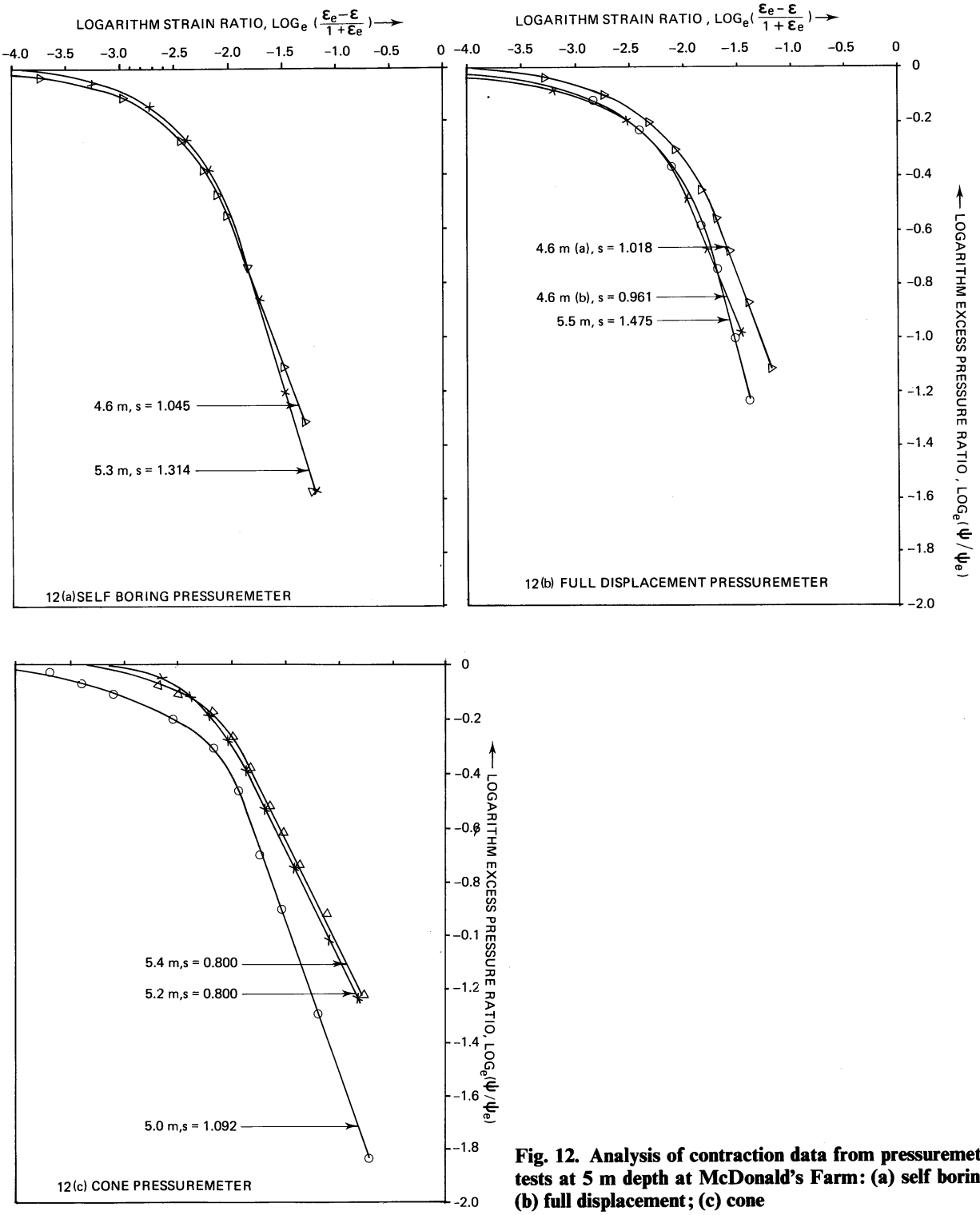

Fig. 12. Analysis of contraction data from pressuremeter tests at 5 m depth at McDonald's Farm: (a) self boring; (b) full displacement; (c) cone

It would appear from Fig. 13 that the value of ϕ' evaluated from the expansion curves is sensitive to the assumed value of ϕ_{cv}'. For example, if ϕ_{cv}' varies by 7° (between 30 and 37°), the deduced value of ϕ' will vary by about 7° also. It would also appear that the value of ϕ' is sensitive to small changes in the slope S_e. Such sensitivity is desirable for reasonable resoluton of the value of ϕ'. A higher value of S_e produces higher values of ϕ', for any selected value of ϕ_{cv}'.

It would appear from Fig. 14 that the value of ϕ' evaluated from the contraction curves is not sensitive to the value of ϕ_{cv}' selected. However, it is not very sensitive to the value of slope S_c, which would imply that the contraction curve is a less sensitive measure of ϕ_v' than the expansion

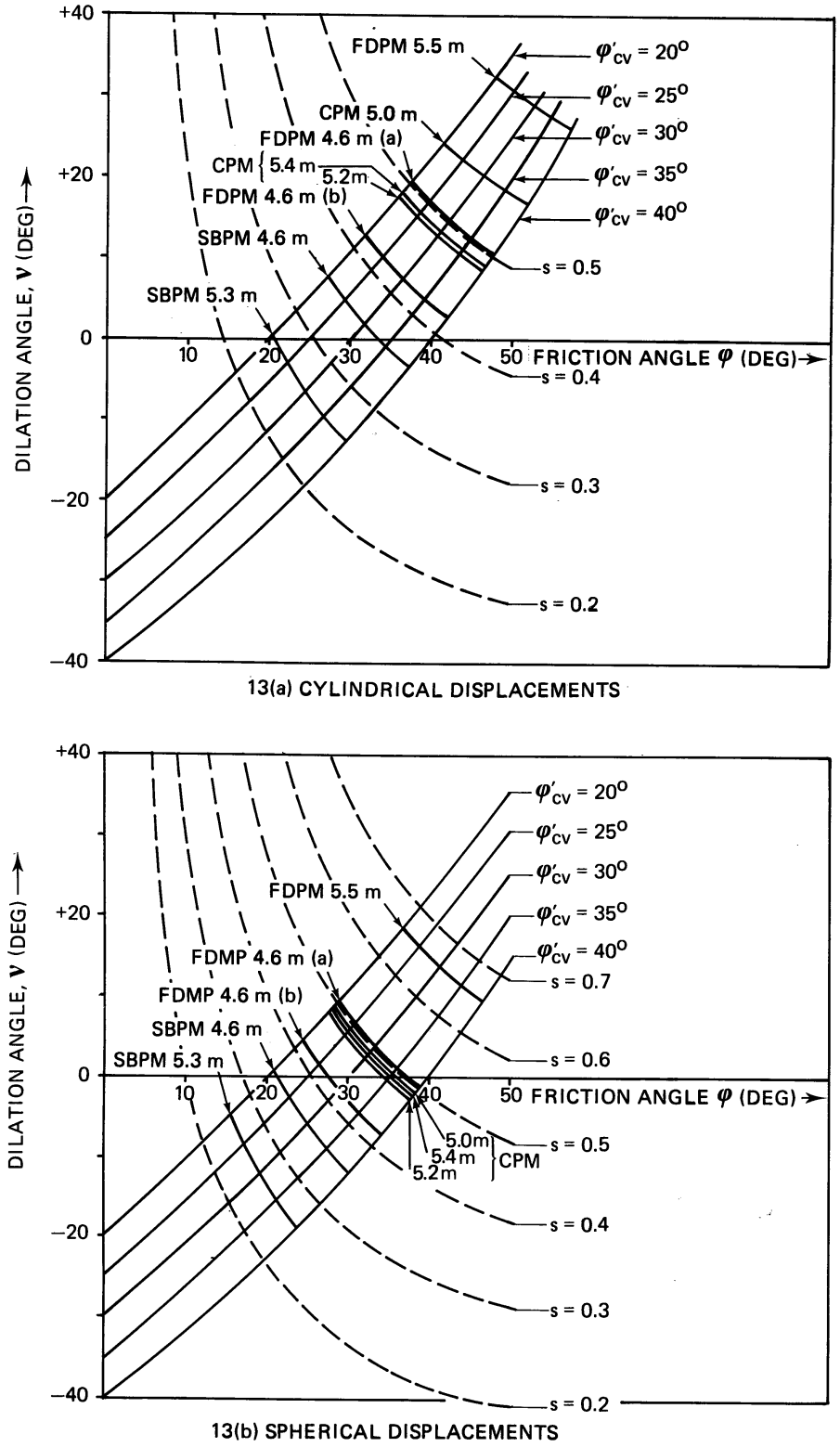

Fig. 13. Nomogram to derive friction and dilation angles from pressuremeter expansion data: (a) cylindrical displacements; (b) spherical displacements

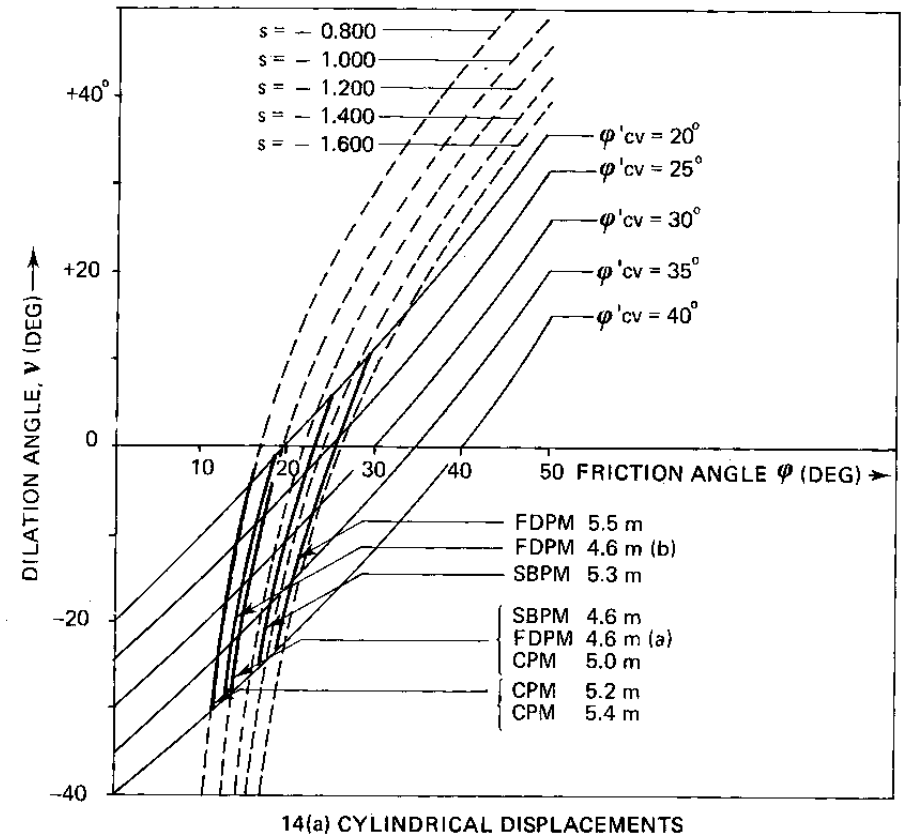

14(a) CYLINDRICAL DISPLACEMENTS

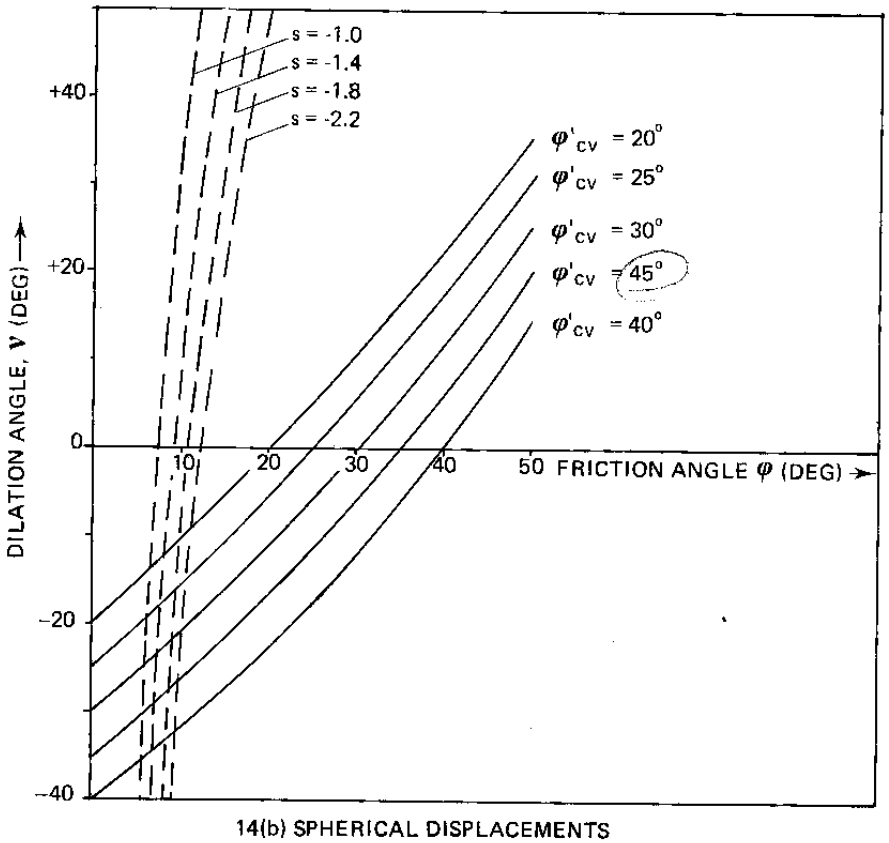

14(b) SPHERICAL DISPLACEMENTS

Fig. 14. Nomogram to derive friction and dilation angles from pressuremeter contraction data: (a) cylindrical displacements; (b) spherical displacements

Table 1. Values of ϕ' and v obtained from pressure–expansion curves

Pressuremeter type	Depth: m	ϕ': deg	v: deg	Expansion model $\phi_{cv}' = 35°$
Self boring pressuremeter	4·6	34·3	−1·0	Cylindrical
	5·3	26·7	−9·5	
Full displacement pressuremeter	4·6 a	39·0	+5·0	
	4·6 b	44·7	+12·5	
	5·5	54·5	+28·0	
Cone pressuremeter	5·0	49·3	+18·7	
	5·2	43·5	+10·7	
	5·4	44·0	+11·0	
Full displacement pressuremeter	4·6 a	22·7	−9·7	Spherical
	4·6 b	26·7	−10·0	
	5·5	32·0	−3·3	
Cone pressuremeter	5·0	29·3	−7·0	
	5·2	26·3	−10·3	
	5·4	26·0	−10·7	

Table 2. Values of ϕ' and v obtained from pressure–expansion curves

Pressuremeter type	Depth: m	ϕ': deg	v: deg	Contraction model $\phi_{cv}' = 35°$
Self boring pressuremeter	4·6	14·5	−21·5	Cylindrical
	5·3	18·0	−19·0	
Full displacement pressuremeter	4·6 a	14·5	+21·5	
	4·6 b	14·0	+22·5	
	5·5	20·5	+16·5	
Cone pressuremeter	5·0	14·5	+12·5	
	5·2	12·7	+24·0	
	5·4	12·7	+24·0	

curve. Tables 1 and 2 summarize the values of ϕ' and v obtained from the expansion and contraction curves for an assumed ϕ_{cv}' of 35°. This value of ϕ_{cv}' was selected purely to provide a consistent basis for comparing the derived friction angles.

Friction angles obtained from expansion curves

Figure 13 and Table 1 show that the cylindrical model of expansion produces unacceptably high values of friction angle from the full displacement and cone pressuremeter, when compared with the values obtained from the self boring pressuremeter and the cone resistances. The Robertson & Campanella (1983) correlation between peak friction angle and cone resistance (which is empirically related to bearing capacity theory) implies friction angles between 35° and 41°.

Also the spherical model of expansion produces unacceptably low values of friction angles from the full displacement and cone pressuremeter, when compared with the values obtained from the conventional cylindrical model of the self boring pressuremeter expansion and the cone resistances.

Friction angles obtained from contraction curves

Figure 14 and Table 2 show that the contraction curves for the self boring, full displacement and cone pressuremeters produce similar values of friction angle, and that the spherical model of contraction produces very much lower friction angles than the cylindrical model.

Comparison of the ϕ' and v values obtained from the expansion and contraction curves show that the contraction curves produce very low values of ϕ' (14·0–20·5°) and negative values of v (−16·5 to −24°), if a ϕ_{cv}' during contraction equal to the ϕ_{cv}' during expansion (=35° in this case) is assumed. These are 9–25° lower than the values obtained from the expansion curves. Even if the soil is presumed to deform at constant volume during contraction ($\phi' = \phi_{cv}'$, $v = 0$), the values of ϕ' only increase to 16·5–25°.

Houlsby *et al.* (1986) also found similarly large differences in the friction angle derived from self boring pressuremeter expansion and contraction curves. The ϕ' values from the contraction curve were 11–26° lower than the ϕ' values from the expansion curve. It was assumed that $\phi' = \phi_{cv}'$ and $v = 0$ during the contraction. Therefore had ϕ_{cv}' during contraction been presumed to be the

same as ϕ_{cv}' during expansion, a slightly greater difference would have resulted.

It would therefore appear that simple cavity contraction models are not suitable to derive friction angles from self boring or full displacement pressuremeter curves. Research is needed to develop a more sophisticated model for use with the repeatable data obtained from the contraction curves.

LIFT OFF PRESSURES

The self boring pressuremeter lift off pressure varies between 100 and 280 kPa. The lift off pressure is sensitive to the disturbance caused by insertion. If insertion generates unintended displacements of 0·1% of the radius of the pressuremeter (i.e. about 0·03 mm only) in soil with a shear modulus of 50 MPa, the lift off pressure could differ by 100 kPa from the zero disturbance value.

The lift off pressures for the full displacement pressuremeter ranges between 90 and 130 kPa. The range for the cone pressuremeter is 50–100 kPa. The gross disturbance generated by the penetration of the full displacement type pressuremeters may paradoxically contribute to the better repeatability of the lift off pressure. The formation of a thin stress relieved zone within an annulus of prestressed stiffer sand (formed by the high mean effective stresses generated by the cone tip penetration) has been postulated by Hughes & Robertson (1985). The magnitude of stress relief is a function of the cone geometry, the stiffness G and normal stresses σ set up in the soil annulus. It is suggested that both G and σ are likely to be proportional to each other. If this is so, then an increased σ, caused by a higher cone resistance, could be offset by a larger stress relief (since G is also larger).

SENSITIVITY OF EXPANSION CURVE TO STRAIN RATE

Constraints on the time available for commercial cone pressuremeter tests impose a need for relatively fast inflation and deflation rates (5–10%/min). These are much higher than those commonly used for other types of pressuremeter (0·5–1%/min).

Allowing creep displacements to occur before the unload–reload loops provides additional information on the sensitivity of the pressure–expansion curve to the expansion rate. For example the records of the variation of the creep displacement with time for the multiple unload–reload loops test at McDonald's Farm or Leidschendam (Fig. 8 shows an example) could be analysed to provide the variation of creep displacement rate with creep displacement. Such data (e.g. Fig. 8b) could be used to construct contours of constant expansion rate curves on the pressure–expansion curve. Such contours would illustrate the sensitivity of the expansion curves to variations in expansion rate and, with appropriate analysis, lead to calculation of the creep properties of the soil.

The pore pressure sensor in the piezocone will indicate if any pore pressures are generated during cone penetration, and if pore pressures are likely to affect the pressuremeter inflation curve.

PROPOSED TEST PROCEDURE

It is desirable to standardize equipment dimensions, accuracies and test procedures in order to compare properly data from different soils. Such comparison will be needed to develop a full understanding of soil response to cone pressuremeter tests and so to extract the maximum information about soil strength–deformation properties.

Based on the experience gained from the various types of pressuremeter tests at McDonald's Farm and at Leidschendam, the following procedure for cone pressuremeter tests is proposed for discussion (Fig. 15).

Once the centre of the pressuremeter membrane has reached the test level selected from the cone profile, the thrust on the cone rods should be removed and membrane inflation should start.

The membrane should be inflated at a fast rate (between 5 and 10%/min). Initially, until the membrane starts to move, inflation should be pressure controlled. Thereafter the inflation rate should be constant until a displacement ($\Delta R/R_0$) of about 5% is reached (A–B in Fig. 15).

The pressure should be held constant to allow creep to occur until the creep displacement rate has decayed to about 0·1%/min. This should take less than 5 min for reasonably clean quartz sand (B–C in Fig. 15). If deflation has to start before the creep rate has reduced to 0·1%/min the initial slope of the unload curve may not provide a realistic measure of shear modulus (C–D–C in Fig. 15).

An unload–reload loop should be carried out. This can perhaps most easily be pressure controlled since the strain increments are small. It is suggested the change in cavity pressure $\Delta\Psi_{ur}$ be limited to $\Delta\Psi_{ur} = 0{\cdot}4\ (\Psi_m - u_0)$, where Ψ_m is the pressure at the start of unloading and u_0 is hydrostatic pressure. This ensures that the circumferential stress remains the minor principal stress for typical granular soils.

The membrane should then be expanded to about 10% cavity strain, at 10%/min (C–E in Fig. 15) and the pressure should then be held constant

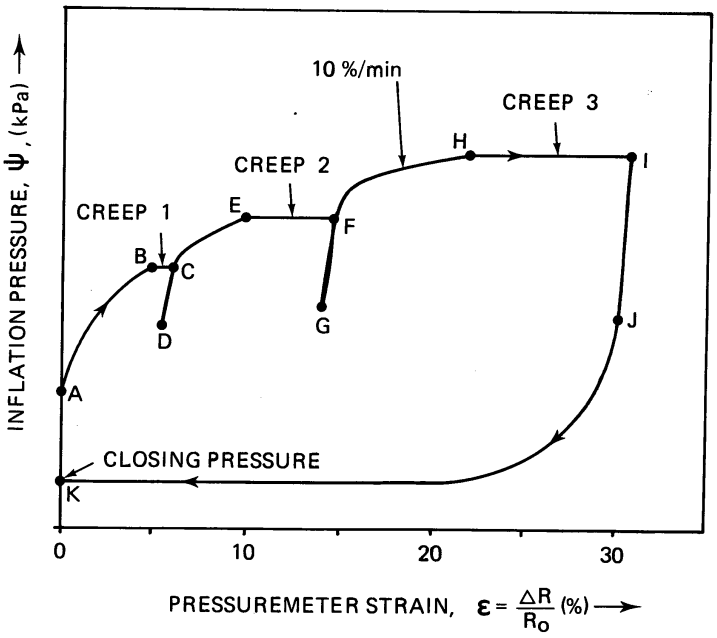

Fig. 15 Proposed test procedure for cone pressuremeter tests in sand

until the expansion rate drops to 0·1%/min as per the third step (E–F in Fig. 15). Up to 5% strain may occur during this holding phase and it may take about 10 min for the rate to decay.

Another unload–reload loop should be performed as per the fourth step (F–G–F in Fig. 15).

Expansion should then continue to between 20–25% average cavity strain (F–H in Fig. 15) and the pressure again held constant. This creep phase (*H–I* in Fig. 15) may require 20 min or more and strains greater than 10% may occur. The average cavity strain should not be allowed to exceed 35% and no single strain arm measurement should be allowed to exceed 45% cavity strain.

Deflation (I–J–K in Fig. 15) should be strain controlled at the same rate as the inflation (5–10%/min) until the membrane collapses back on to the body of the membrane. This test procedure will provide data with which to determine

(*a*) the shear modulus G at three different expansions ξ_m and pressures Ψ_m
(*b*) the sensitivity of the inflation curve to inflation rate and the creep properties of the soil
(*c*) the angle of friction ϕ and dilation, v, of the soil (once suitable analyses have been developed).

CONCLUSIONS FOR DERIVATION OF SHEAR MODULUS AND FRICTION ANGLE

The following conclusions can be made.

(*a*) The procedures for determining shear modulus produce values in good agreement with those from other tests.
(*b*) The resolution of the available data and the theoretical analysis are not sufficiently developed to quantify the variation of shear modulus with stress Ψ_m and strain increment $\Delta\xi$ within the unloading loops.
(*c*) Complete explanations for the large creep displacements in the relatively clean quartz sand at McDonald's Farm and Leidschendam need to be developed.
(*d*) Cavity expansion and contraction models are not yet suitable to determine friction angle from full displacement pressuremeter tests Further research is needed to develop more realistic models of the displacement and stress fields around the pressuremeter, before derivation of reliable friction and dilation from the loading and unloading curves becomes possible.
(*e*) The repeatability of the data, particularly that of the unloading curves, encourages the belief that the cone pressuremeter has the potential to provide reliable measures of friction and dilation angle.

CONCLUSIONS FOR APPLICATION OF CONE PRESSUREMETER DATA

The good comparison between the values of shear modulus obtained from cone pressuremeter tests and values from self boring pressuremeter and seismic tests suggest that the cone pressuremeter can be used to provide profiles of reliable shear moduli for use in foundation analysis.

Improvement to the resolution of displacement measurements in the next generation of cone pressuremeters will enable in situ data to be col-

lected to evaluate the suitability of the cone pressuremeter to provide a measure of the variation of the shear modulus with strain level (for use in hyperbolic stress–strain models).

The creep potential of sand under sustained loading evaluated by cone pressuremeter tests may find application in calculations of long-term foundation behaviour once the significance of the cone pressuremeter data has been evaluated. In the interim the cone pressuremeter can be used to provide comparative measures of creep potential in different soils.

The in situ measurements of dilation and friction angle with the cone pressuremeter and the easy construction of profiles of dilation and friction angle using the cone data will find wide application once suitable analytical procedures have been established.

Robertson *et al.*, (1986) have illustrated the use of FDPMT data in the derivation of P–Y curves for the analysis of lateral loading of piles. The effect of strain rate will be negligible for small deflections, but may be important at larger deflections. In this case, the insertion of the probe is a model of the installation of a pile.

In addition to the above procedure, Robertson (1982) and Brown (1985) have illustrated the use of cyclic loading in pressuremeter tests to indicate the potential for accumulated strain under repeated loading. This may have applicability for analysis of soil behaviour during earthquake loading.

Research is continuing at Oxford University and the University of British Columbia into the interpretation and use of cone pressuremeter tests. Areas of interest include the use of the final unloading portion of the test to determine soil friction and dilation angles and the significance of the observed creep behaviour. Simultaneously, development of the next generation of equipment by Fugro and by UBC is proceeding.

ACKNOWLEDGEMENTS

The Authors are grateful to Fugro Geotechnical Engineers and Fugro Geotechniek, which provided the essential cone pressuremeters. They also supported the tests at Leidschendam and the preparation of this Paper. The University of British Columbia provided invaluable technical support to the field work at McDonald's Farm as part of the ongoing programmes of research of in situ testing tools and of development of their seismic cone pressuremeter.

The assistance of Dr G. T. Houlsby of Oxford University, who provided valuable criticism, is much appreciated. The work of Mr F. Gozeling on data reduction is also appreciated.

REFERENCES

1. Baguelin, F. J. & Jezequel, J.-F. (1983). The LPC Pressio Penetrometer. *Proc. Symp. on Geotechnical practice in offshore engineering.* Austin, Texas.
2. Baligh, H. M. (1986). Undrained deep pentration, I: Shear stress, and II: Pore pressures. *Géotechnique* **36,** No. 4, 471–502.
3. Brown, P. T. (1985). *Predicting laterally loaded pile capacity using the pressuremeter.* MASc thesis, University of British Columbia, Vancouver.
4. Houlsby, G. T., Clarke, B. G. & Wroth, C. P. (1986). Analysis of the unloading of a pressuremeter in sand. *Proc. Symp. Pressuremeter and its Marine applications.* ASTM STP 950. pp. 245–262.
5. Hughes, J. M. O., Wroth, C. P. & Windle, D. (1977). Pressuremeter tests in Sands, *Géotechnique* **27,** No. 4, 455–477.
6. Hughes, J. M. O. (1982). Interpretation of pressuremeter tests for the determination of elastic shear modulus. *Engineering foundation conf. on updating subsurface sampling of soils and rocks and their in-situ testing.* Santa Barbara, California.
7. Hughes, J. M. O. & Robertson, P. K. (1985). Full displacement pressuremeter testing in sand. *Can. Geotech. J.* **22,** No. 3, 298–307.
8. Kay, S. J., Griffiths, D. V. & Kolk, H. J. (1986). Application of pressuremeter testing to assess lateral pile response in clays. *Proc. Symp. Pressuremeter and its marine applications.* **ASTM** STP 950, pp. 458–477.
9. Robertson, P. K. (1982). *Insitu testing of soil with emphasis on its application to liquefaction assessment.* PhD. thesis, University of British Columbia, Vancouver.
10. Robertson, P. K. & Campanella, R. G. (1983). Interpretation of cone penetration tests part 1: sand. *Can. Geotech. J.* **20,** No. 4, 718–733.
11. Robertson, P. K., Hughes, J. M. O., Campanella, R. G., Brown, P. & McKeown, S. (1986). The design of laterally loaded piles using the pressuremeter. *Proc. Symp. on Pressuremeter and its marine applications.* **ASTM** STP 950, pp. 443–457.
12. Rowe, P. W. (1962). The stress–dilatancy relation for static equilibrium of an assembly of particles in contact, *Proc. R. Soc. A* **269,** 500–527.
13. Vaid , Y. P. & Campanella, R. G. (1977). Time dependent behaviour of undisturbed clay. *J. Geotech Engng Div.* **181,** GT7, 693–709.
14. Withers, N. J., Schaap, L. H. J. & Dalton, J. C. P. (1986). The development of a full displacement pressuremeter. *Proc. Symp. on Pressuremeter and its marine applications.* ASTM STP 950, pp. 38–56.